Textureless Macula Swelling Detection With Multiple Retinal Fundus Images

Luca Giancardo*, *Student Member, IEEE*, Fabrice Meriaudeau, *Member, IEEE*,
Thomas P. Karnowski, *Member, IEEE*, Kenneth W. Tobin Jr., *Senior Member, IEEE*, Enrico Grisan, *Member, IEEE*,
Paolo Favaro, *Member, IEEE*, Alfredo Ruggeri, *Senior Member, IEEE*, and Edward Chaum, *Member, IEEE*

Abstract—Retinal fundus images acquired with nonmydriatic digital fundus cameras are versatile tools for the diagnosis of various retinal diseases. Because of the ease of use of newer camera models and their relatively low cost, these cameras can be employed by operators with limited training for telemedicine or point-of-care (PoC) applications. We propose a novel technique that uses uncalibrated multiple-view fundus images to analyze the swelling of the macula. This innovation enables the detection and quantitative measurement of swollen areas by remote ophthalmologists. This capability is not available with a single image and prone to error with stereo fundus cameras. We also present automatic algorithms to measure features from the reconstructed image, which are useful in PoC automated diagnosis of early macular edema, e.g., before the appearance of exudation. The technique presented is divided into three parts: first, a preprocessing technique simultaneously enhances the dark microstructures of the macula and equalizes the image; second, all available views are registered using nonmorphological sparse features; finally, a dense pyramidal optical flow is calculated for all the images and statistically combined to build a naive height map of the macula. Results are presented on three sets of synthetic images and two sets of real-world images. These preliminary tests show the ability to infer a minimum swelling of 300 μm and to correlate the reconstruction with the swollen location.

Index Terms—Biomedical image processing, diabetes, image motion analysis, image reconstruction, image registration, medical diagnostic imaging, stereo image processing.

*L. Giancardo is with Le2i, University of Burgundy, 71200 Le Creusot, France, and also with the Oak Ridge National Laboratory, Oak Ridge, TN 37831 USA (e-mail: giancardol@ornl.gov).

F. Meriaudeau is with Le2i, University of Burgundy, 71200 Le Creusot, France (e-mail: fabrice.meriaudeau@u-bourgogne.fr).

T. P. Karnowski and K. W. Tobin, Jr., are with the Oak Ridge National Laboratory, Oak Ridge, TN 37831 USA (e-mail: karnowskitp@ornl.gov; tobinkwjr@ornl.gov).

E. Grisan and A. Ruggeri are with the BioImLab, University of Padua, 35122 Padova, Italy (e-mail: enrigri@dei.unipd.it; alfredo.ruggeri@unipd.it).

P. Favaro is with the Heriott-Watt University, Edinburgh, EH14 4AS, U.K. (e-mail: p.favaro@hw.ac.uk).

E. Chaum is with the University of Tennessee Health Science Center, Memphis, TN 38163 USA (e-mail: echaum@uthsc.edu).

Color versions of one or more of the figures in this paper are available online at http://ieeexplore.ieee.org.

Digital Object Identifier 10.1109/TBME.2010.2095852

I. INTRODUCTION

DIGITAL fundus cameras are becoming the norm in ophthalmologist practices, but they are also becoming more common in point-of-care (PoC) facilities such as walk-in clinics. Modern nonmydriatic retinal imaging platforms have many standard features to assist in ease of use and high throughput. Since 2005, our group has been designing, developing, and testing a semiautomated, Health Insurance Portability and Accountability Act (HIPAA) compliant, teleophthalmology network for the screening of diabetic retinopathy and related conditions in under served regions of the mid-South U.S. Currently, five clinics utilize nonmydriatic fundus cameras modified to automatically send pictures and patients' metadata to our central server for a diagnosis [1].

The ease of use, relatively low cost, and utility of these instruments in detecting various retinal diseases make them ideal for this application. However, there are many cases when the 3-D structure of the retina would be useful or even essential for a correct diagnosis. This is especially the case for the initial stages of diabetic macular edema (DME), a common cause of vision loss and blindness [2]. DME occurs in the retina of diabetic patients due to leakage of fluid within the macula, which creates diffuse swelling and cystic changes that are not immediately visible with monocular fundus images. The classical way to detect this fluid is either by waiting for its absorption, which turns into exudation or by analyzing the 3-D shape of the outer layer of the retina (with particular focus in the macula area).

Typically, the 3-D information is obtained with stereoscopic fundus cameras or optical coherence tomography (OCT) instruments. However, stereo glasses are required to visualize the depth field in commercially available stereoscopic fundus cameras. Hence, they do not extract numerical information that can be used as features in automatic methods and are prone to substantial intra/interreader variability on the diagnosis [3]. This is a serious drawback for their use in automatic diagnosis of macula swelling. The ideal solution, a OCT system in conjuction with a fundus camera, has considerable cost disadvantages and requires additional training for the operators who will be capturing the images. This seriously limits its practicality in a PoC environment. Thus, an algorithm able to infer the 3-D shape of the retina from multiple fundus cameras images would be extremely beneficial in terms of cost, and also can add capabilities for automatic diagnosis of fluid leakage in the macula area, which can be invisible in standard fundus images [see Fig. 4(a)]. We note that obtaining multiple images is rather simple with modern high-quality, easy-to-use general-purpose

fundus cameras, as the image acquisition time is fast (a few seconds for each) and painless for the patient.

In the literature, there are examples of 3-D retina reconstruction algorithms that concentrate mainly on optic nerve reconstruction for the detection of glaucoma, either with a calibrated stereoscopic fundus camera [4]–[6] or with multiple views from a standard monocular fundus camera [7], [8], provided that the aperture of the monocular camera is kept smaller than the eye pupil [9]. Choe *et al.* present a reconstruction technique on the entire field of view (FOV) of the image employing fluorescein images, which require a special filter on the fundus camera and the injection of a contrast agent, a technique that is too invasive for screening purposes and that cannot be performed outside a specialized clinic due to possible unwanted secondary effects [10]. However, to our knowledge, no research group has proposed any method to directly identify swelling of the macula (an almost textureless area of the retina) with fundus images. The lack of a fixed multiview configuration for the PoC fundus cameras and the impracticality of a calibration procedure are a difficult but common problem in 3-D multiview geometry. There are various approaches that are able to successfully tackle this problem, such as bundle adjustment/structure from motion [11] or simultaneous localization and mapping (SLAM) [12]. All these techniques require strong salient point correspondences to simultaneously estimate the camera pose and the 3-D structure. This is not possible in the macula, which has little texture and where "corners" cannot be reliably tracked and matched.

We propose a novel algorithm able to identify macular swelling through the reconstruction of a naive height map of the macula area from multiple fundus images with an unknown translation (roughly parallel to the eye), captured by an uncalibrated fundus camera. In our experiments, we show how retina "blisters" can be identified, even in areas where there is no apparent texture visible using four fundus images.

II. IMAGING IN A TELEMEDICINE OR POC SETTING

Modern nonmydriatic retinal imaging platforms are made with automatic focusing and positioning aids, software guidance, real-time display, and automated illumination to assist in ease of use and high throughput. The patient sits before the camera with a comfortable headrest. No pupil dilation is used. Programmed sequences and freely positionable eye fixation targets are available to permit steady image acquisition from different points of view. This allows the acquisition of four retina images in less than a minute. The camera is connected to an integrated personal computer with patient databases and built-in Internet connectivity. In our telemedical network application, software has been installed on the camera computer to remotely upload the current shot to a central image processing server. The server executes the algorithm described in this letter (in addition to other software for quality estimation and automatic diagnosis developed by our group) and generates a clinical report. The report is immediately accessible via a secure Web connection that has been verified and validated on standard and mobile internet clients (an overview of the complete existing system is available in [1]). We note that in a more advanced system, the diagnosis
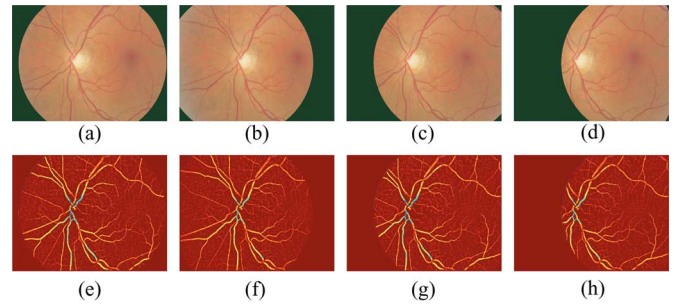
Fig. 1. (a)–(d) Images captured with the virtual fundus camera. (e)–(h) Images after the preprocessing phase.

could be done on the camera computer without the need of a central server.

III. MATERIALS

The development and testing of our algorithms requires a gold standard for comparison with the reconstruction (i.e., a profile from an OCT instrument) and images of patients with blisters of different heights. The collection of this type of data is a challenging task by itself; hence, to speed up the development phase and to improve the evaluation, we have developed and tested the algorithm with a faithful ray-traced model of the camera–eye–retina system. We have made this model and related software available online (see http://vibot.u-bourgogne.fr/luca/). The optical model was initially designed in Zemax to create a credible representation of fundus camera/optical eye structure and then modeled in POVray, a freely available ray-tracing tool. In our model, we place a real image of the retina fundus at the back of the eye and extrude it with a given height map that acts as a ground truth. We acquired four virtual shots by laterally translating the camera at $10°$, $5°$, $-5°$, and $-10°$ (the angle is calculated between the centers of the objective lens and the cornea). Fig. 1(a)–(d) shows the examples of the images obtained by translating the virtual camera. The resolution used is 1024×768.

In order to acquire preliminary data on the clinical viability of the method, we asked a camera operator to obtain four images with the only constraint being lateral translation between the images. The operator acquired two sets of images from two patients with associated OCT data for verification. One patient shows a blister in the OCT image, which is invisible to the fundus camera [see Fig. 4(a)], while the other has a completely healthy macula [see Fig. 5(a)]. The operator translated the camera a considerably smaller amount than the translation present in the simulated images (estimated at 10%), which reduces the baseline and makes the reconstruction more challenging, but provided an interesting testbed for these preliminary experiments.

IV. METHOD

The reconstruction algorithm is divided into three phases: *preprocessing*, *registration*, and *naive-height-map reconstruction*. First, the fundus images are enhanced to remove background

information and reflections from the nerve fiber layer. This step also enhances the microstructures in the macula area. Second, all images are rigidly registered by employing fiducial points independent of retina morphology. Finally, the naive height map is reconstructed exploiting the statistical distribution of a dense optical flow analysis between images.

1) Preprocessing: We start the preprocessing by extracting the green channel I_g from each image and performing an initial estimation of the background by means of a large square median filter whose size is $1/30$ the vertical size of the fundus image. This estimation is enhanced with the addition of a morphological reconstruction step [13]. The estimated background is subtracted from the original image with 16-bit signed precision to maintain negative pixel values. The image obtained shows a distinct gray-level distribution: the highest peak of the histogram is always centered on zero regardless of the ethnicity of the patient, disease, or point of view of the camera [14]. We are able to obtain the texture-enhanced version of the macula, as shown in Fig. 1, by maintaining the absolute value of the negative pixel values only. With this technique, we are able to remove most of the illuminations changes due to the different positions of the camera.

2) Registration: The motion between fundus images is compensated through a registration technique inspired by Cattin *et al.* [15] using speeded up robust features (SURFs) [16], a local descriptor that can quickly generate an informative 64-D vector for a given point. We selected the salient points with a SURF quality value greater than 0.0001. Then, all salient points are matched throughout all views employing the Euclidean distance between SURF vectors. Only the points showing a distance ratio (*best match/second best match*) larger than 0.7 are kept. The RANSAC algorithm with rotational homography is used to estimate the outliers (i.e., the points whose geometry is unfit for the rotational rigid transformation) [11]. The common FOV is detected with the method described in [17].

3) Naive-Height-Map Reconstruction: The reconstruction of the macular shape is based on the fact that most of the retinal structures have a very small height (<0.8 mm) in comparison to the planar size of the retina; hence, the rigid registration allows a nearly perfect alignment of most of the areas apart from the ones closer to the camera, i.e., blisters. We exploit this characteristic by building $n - 1$ disparity maps, where n is the number of images and each map is built using a common reference image identified as im_0, i.e., $\text{im}_0 \leftrightarrow \langle \text{im}_1, \ldots, \text{im}_{n-1} \rangle$. Because of the lack of strong salient points in the macula, the disparity maps are approximated by computing the dense optical flow with the pyramidal Lucas–Kanade method [18], for each pixel of the image (in the common FOV) with a window of 19 pixels and 3 pyramids. The magnitude of each vector is computed in order to obtain the provisional disparity maps $\langle \text{im}_1^{\text{dmap}}, \ldots, \text{im}_{n-1}^{\text{dmap}} \rangle$.

Assuming that in the areas where there is no texture, the flow vector obtained will be random, while in the areas with little texture the noise will be normally distributed, we can compute a final naive height map im^{nhm} as follows:

$$\text{im}^{\text{nhm}} = \frac{1}{n-1} \sum_{i=1}^{n-1} \text{im}_i^{\text{dmap}}. \tag{1}$$
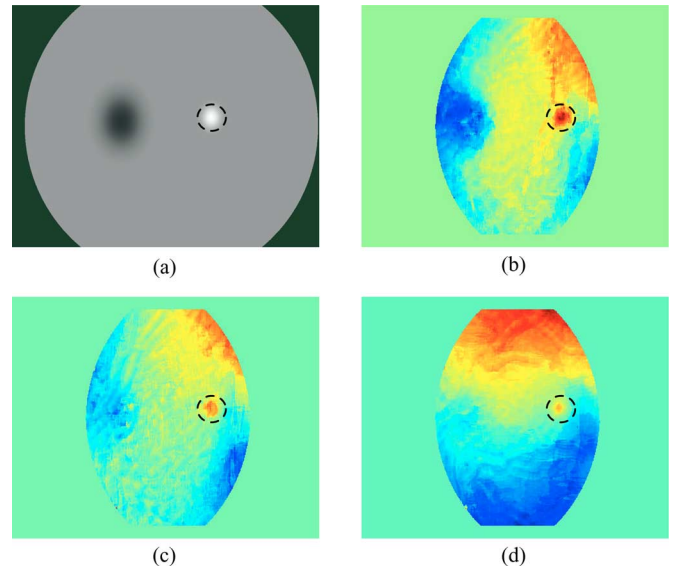
Fig. 2. (a) Synthetic height map used to generate the retina 3-D structure (the white spot represents the blister). (b)–(d) Reconstructed naive height maps containing a blisters of decreasing height, respectively, 0.5, 0.4, and 0.3 mm. The area contained by the dashed circle shows the position of the original blister.
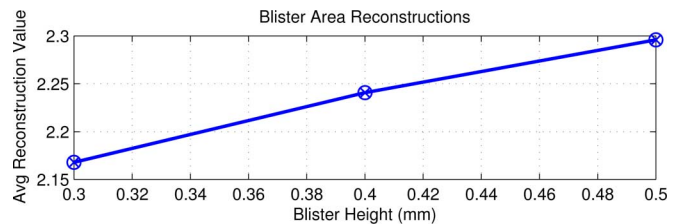
Fig. 3. Mean value of the reconstructed naive height map in the area shown in Fig. 2 for the different heights of the blisters generated with the virtual camera.

V. RESULTS AND CONCLUSION

Using the images generated with the virtual camera, it was possible to reconstruct the exact position of the blister in the macular area as shown in Fig. 2. In Fig. 3, we show the reconstruction ability numerically by calculating the mean of the naive-height-map value in the same area. In the experiment, this value linearly correlates with the height of the blister.

Figs. 4 and 5 show the algorithm's reconstruction ability on the images acquired by the operator as described in Section III. Based on the fundus images alone, these patients do not exhibit any abnormality. In Figs. 4(b) and 5(b), we show the reconstructed naive height maps, and in Figs. 4(c) and 5(c), we show the 3-D overlay of the reconstruction with the accompanying OCT. Although the reconstruction has a lower quality than the simulated images of Fig. 2, the healthy macula is clearly discernible from the swollen one. The 3-D construction overlay [see Fig. 5(c)] demonstrates a strong correlation with the actual retina edema seen on OCT imaging. The difference in average height in the macula area between the healthy and nonhealthy image is 2.13, a result that (if confirmed by further experiments) will be a clinically significant value for the automated detection of macular swelling. We were able to analyze a set of four

is a key indicator of the early phases of diseases such as DME. Multiview image reconstruction can be used to perform 3-D reconstructions, but the lack of strong salient feature points in the macula is a potential flaw in many existing multiview reconstruction approaches. In this study, we have presented a method that performs a straightforward statistical analysis of noisy disparity maps to generate a naive height map that can be used to display and potentially measure blisters in the macular area. We have shown its feasibility on synthetic images constructed using a computer model and have also illustrated its effectiveness on two datasets of four fundus images and associated OCT data. The proposed algorithm is a promising addition to automated image analysis using inexpensive fundus cameras well-suited to PoC and telemedical applications.

Fig. 4. Patient A. (a) Real fundus image of a patient with a blister invisible to a standard fundus camera. (b) Reconstructed map showing the blister; the white circle shows the area of interest. (c) OCT image of the highlighted area with a red overlay of the 3-D reconstruction obtained.
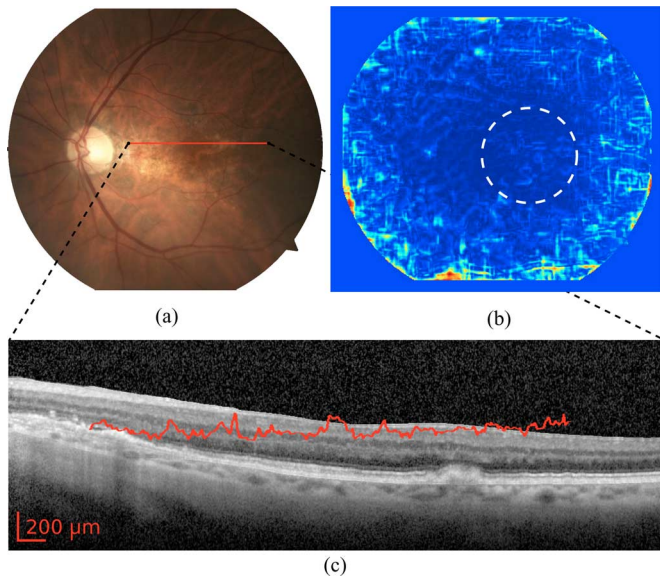
Fig. 5. Patient B. (a) Real fundus image of a patient with a healthy macula. (b) Reconstructed map, the white circle shows the area of interest. (c) OCT image of the highlighted area with a red overlay of the 3-D reconstruction obtained.

images in under 5 min on a 2.2-GHz machine with 4-GB memory using a MATLAB algorithm implementation.

In the reconstructions, we notice artifacts of increasing strength starting roughly outside the macula area. They are due to lens distortions and miscalculation of the optical flow; however, these are not a problem because our algorithm is focused on the macular area, which can be automatically identified by other image-processing algorithms [19].

In conclusion, fundus camera is an effective tool for diagnosis of retinal diseases, but cannot reliably detect depth, which

REFERENCES

[1] Y. Li, T. P. Karnowski, K. W. Tobin, L. Giancardo, and E. Chaum. (2009, Apr.). "A network infrastructure for automated diagnosis of diabetic retinopathy," in *Proc. Amer. Telemed. Assoc. Annu. Meeting*, [Online]. Available: http://vibot.u-bourgogne.fr/luca/papers/Li2009.pdf

[2] D. E. Singer, D. M. Nathan, H. A. Fogel, and A. P. Schachat, "Screening for diabetic retinopathy," *Ann. Int. Med.*, vol. 116, no. 8, pp. 660–671, Apr. 1992.

[3] H. K. Li, L. D. Hubbard, R. P. Danis, A. Esquivel, J. F. Florez-Arango, and E. A. Krupinski, "Monoscopic vs. stereoscopic retinal photography for grading diabetic retinopathy severity," *Invest. Ophthalmol. Vis. Sci.*, vol. 51, no. 6, pp. 3184–3192, Jun. 2010.

[4] E. Corona, S. Mitra, M. Wilson, T. Krile, Y. H. Kwon, and P. Soliz, "Digital stereo image analyzer for generating automated 3-d measures of optic disc deformation in glaucoma," *IEEE Trans. Med. Imag.*, vol. 21, no. 10, pp. 1244–1253, Oct. 2002.

[5] J. Xu and O. Chutatape, "Auto-adjusted 3-d optic disk viewing from low-resolution stereo fundus image," *Comput. Biol. Med.*, vol. 36, no. 9, pp. 921–940, Sep. 2006.

[6] T. Nakagawa, T. Suzuki, Y. Hayashi, Y. Mizukusa, Y. Hatanaka, K. Ishida, T. Hara, H. Fujita, and T. Yamamoto, "Quantitative depth analysis of optic nerve head using stereo retinal fundus image pair," *J. Biomed. Opt.*, vol. 13, no. 6, pp. 064026-1–064026-10, 2008.

[7] T. Chanwimaluang, G. Fan, G. G. Yen, and S. R. Fransen, "3-d retinal curvature estimation," *IEEE Trans. Inf. Technol. Biomed.*, vol. 13, no. 6, pp. 997–1005, Nov. 2009.

[8] D. Liu, N. B. Wood, X. Y. Xu, N. Witt, A. D. Hughes, and T. SAMcG, "Advances in Computational Vision and Medical Image Processing," in *3D Reconstruction of the Retinal Arterial Tree Using Subject-Specific Fundus Images*. New York: SpringerLink, 2008, pp. 187–201.

[9] M. Martinello, P. Favaro, G. D. Muyo Nieto, A. R. Harvey, E. Grisan, F. Scarpa, and A. Ruggeri, "3-d retinal surface inference: Stereo or monocular fundus camera?" in *Proc. EMBS*, 2007, pp. 896–899.

[10] T. E. Choe, I. Cohen, and G. Medioni, "3-d shape reconstruction of retinal fundus," in *Proc. IEEE Comput. Soc. Conf. Comput. Vis. Pattern Recognit.*, 2006, vol. 2, pp. 2277–2284.

[11] R. Hartley and A. Zisserman, *Multiple View Geometry in Computer Vision*. Cambridge, U.K.: Cambridge Univ. Press, 2003.

[12] H. Durrant-Whyte and T. Bailey, "Simultaneous localisation and mapping (slam): Part I—The essential algorithms," *Robot. Autom. Mag.*, vol. 13, no. 2, pp. 99–110, 2006.

[13] L. Vincent, "Morphological grayscale reconstruction in image analysis: Applications and efficient algorithms," *IEEE J. Image Process.*, vol. 2, no. 2, pp. 176–201, Apr. 1993.

[14] L. Giancardo, E. Chaum, T. P. Karnowski, F. Meriaudeau, K. W. Tobin, and Y. Li, "Bright retinal lesions detection using color fundus images

containing reflective features," in *Proc. World Congr. Med. Phys. Biomed. Eng.*, 2009, pp. 292–295.

[15] P. C. Cattin, H. Bay, L. V. Gool, and G. Szekely, "Retina mosaicing using local features.," *Med. Image Comput. Comput. Assist. Intervent.*, vol. 9, no. 2, pp. 185–192, 2006.

[16] H. Bay, A. Ess, T. Tuytelaars, and L. Van Gool, "Surf: Speeded up robust features," *Comput. Vis. Image Understand.*, vol. 110, no. 3, pp. 346–359, 2008.

[17] L. Giancardo, F. Meriaudeau, T. P. Karnowski, E. Chaum, and K. Tobin, "New developments in biomedical engineering," *Quality Assessment of Retinal Fundus Images Using ELVD*, Croatia:IN-TECH, pp. 201–224, 2010.

[18] J. Bouguet, "Pyramidal implementation of the lucas kanade feature tracker description of the algorithm," Intel Corporation, Microprocessor ResearchTech. Rep., 2000.

[19] K. W. Tobin, E. Chaum, V. P. Govindasamy, and T. P. Karnowski, "Detection of anatomic structures in human retinal imagery.," *IEEE Trans. Med. Imag.*, vol. 26, no. 12, pp. 1729–1739, Dec. 2007.